Two-Port Indirect Acoustic Impedance eduction in presence of grazing flows

Conference Paper · June 2011

DOI: 10.2514/6.2011-2868

4 authors:

Leandro D. Santana
University of Twente
15 PUBLICATIONS **42** CITATIONS
SEE PROFILE

Wim De Roeck
University of Leuven
49 PUBLICATIONS **232** CITATIONS
SEE PROFILE

Wim Desmet
University of Leuven
611 PUBLICATIONS **4,046** CITATIONS
SEE PROFILE

Piergiorgio Ferrante
University of Leuven
19 PUBLICATIONS **80** CITATIONS
SEE PROFILE

17th AIAA/CEAS Aeroacoustics Conference (32nd AIAA Aeroacoustics Conference)
05 - 08 June 2011, Portland, Oregon

AIAA 2011-2868

Two-Port Indirect Acoustic Impedance eduction in presence of grazing flows

Leandro D. Santana * , Wim De Roeck* and Wim Desmet *
K.U. Leuven, Department of Mechanical Engineering, Leuven, Belgium

Piergiorgio Ferrante †
Alenia Aermacchi S.p.A., Venegono Superiore, VA, Italy

Aero-engine duct noise control is one of the challenging topics to be solved in view of a more environment friendly civil aviation. The recent developments of advanced acoustic liners require high accuracy on acoustic impedance determination, especially, in presence of flows. This paper presents an analytical methodology for acoustic impedance eduction in presence of grazing flow, based on a two-port representation of an acoustic system. This procedure is dedicated to the frequency range below the cut-on frequency of the transversal duct modes. The methodology is validated by results comparison with acoustic finite element solution, where a known acoustic impedance is imposed to one wall of a rectangular section duct. After the computational validation, the acoustic impedance of two aero-engine acoustic liner samples are experimentally identified and the results are compared with independently obtained impedance curves, showing good agreement. Finally, a sensitivity analysis to the influence of the input parameters is conducted.

I. Introduction

One of the challenges in the design of acoustic liners used in commercial aircraft nacelles is the accurate acoustic impedance deduction under flow conditions. Both direct and indirect techniques are used to measure the acoustic liner impedance. The most commonly used method for determining the acoustic impedance under normal incidence conditions, only applicable for no flow conditions, is the two microphones method.[1] An extensively used direct technique is the in-situ technique.[2] This method assumes that for a resonant cavity, a relationship between the acoustic pressure inside the cavity and the acoustic particle velocity, it is also assumed that the particle velocities on both sides of the perforated plate are identical. In this way, the only quantity to be measured is the transfer function between the acoustic liner surface and the acoustic pressure inside the cavity. The microphones are mounted flush to the back-plate inside the cavity and to the perforated plate. This technique is valid under the hypothesis of a locally reacting liner and long wavelengths compared with the cavity cross dimensions. In addition, this technique is intrusive and requires a cumbersome installation. In contrast with the direct methods, the Mode-Matching Technique[3] is a promising tool for acoustic impedance eduction of materials. This technique executes a modal decomposition of the acoustic pressure and velocity which can be mathematically written as a set of algebraic equations. The acoustic pressure and velocities, measured by an array of microphones focused at the same cross section as the sample, permits the determination of multiple propagation modes on the duct leading to a precise determination of the acoustic impedance. This technique allows to measure the acoustic impedance up to high frequencies but using a large number of microphones.

As an alternative to the techniques mentioned above, the present paper studies an analytical method for acoustic impedance eduction based on a two-port formulation. Under the validity of the assumption of plane wave propagation, this technique allows acoustic impedance deduction, under grazing flow conditions, using a minimum of four microphones. Furthermore, this technique is able to determine the rigid-/impedance-wall transition effect and consequently excludes this effect from the material acoustic impedance, resulting in an accurate acoustic impedance prediction.

This paper the technique is presented theoretically and validated using a comparison with results obtained by an acoustical finite element method. Afterwards, experiments are conducted on two liner samples with

acoustic impedances obtained by a different methodology and the results are compared. Finally, a sensitivity analysis shows the influence of the input parameters on the educed impedance.

II. Acoustic two-port systems

A. The linear acoustic network

A two-port network,[4] represented in figure 1, is defined as an acoustic system localized between two straight ducts where the acoustic plane wave propagation hypothesis is valid. A two-port system is fully characterized by an acoustic transfer matrix (T) which can be written as a relation between the pressure and velocities on each side of the two-port system. Among the several approaches to write the transfer matrix, this paper adopts two representations: one which relates the right and left-running acoustic waves (p^+, p^-) on both sides of the system, the so called scatter matrix T_s, and the other which relates the acoustic pressure and velocities (p, u) on each side of the two port systems. These two representations are, respectively, described by the equations 1 and 2.

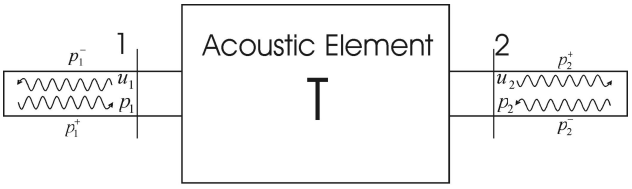

Figure 1. Acoustic two-port system representation.

$$\begin{Bmatrix} p_2^+ \\ p_1^- \end{Bmatrix} = [T_s] \begin{Bmatrix} p_1^+ \\ p_2^- \end{Bmatrix} = \begin{bmatrix} T^+ & R^- \\ R^+ & T^- \end{bmatrix} \begin{Bmatrix} p_1^+ \\ p_2^- \end{Bmatrix} \tag{1}$$

$$\begin{Bmatrix} p(l) \\ u_z(l) \end{Bmatrix} = [T] \begin{Bmatrix} p(0) \\ u_z(0) \end{Bmatrix} = \begin{bmatrix} T_{11} & T_{12} \\ T_{21} & T_{22} \end{bmatrix} \begin{Bmatrix} p(0) \\ u_z(0) \end{Bmatrix} \tag{2}$$

In equation 1, the indexes 1 and 2 represent, respectively, the upstream and the downstream end of the two-port system. In equation 2, the indexes 0 and l respectively represent the plane upstream and downstream where the transition rigid-/impedance wall occurs. De Roeck[5] presents a formulation which uniquely relates the equations 1 and 2.

B. The upstream and the downstream propagating waves

A minimum of two microphones is needed to define the complex upstream (p^+) and downstream (p^-) propagating waves. Assuming plane wave propagation, for an arbitrary fixed reference position $z = 0$, the right- and the left-running acoustic pressure field is directly linked to the reference axial position z by the relationship:

$$p'(z,f) = p^+(z,f) + p^-(z,f) = p^+(0,f)\, e^{-jk^+ z} + p^-(0,f)\, e^{jk^- z}, \tag{3}$$

where the right- and the left-running acoustic wave numbers are defined, respectively, as $k^+ \approx k_0/(1-M)$ and $k^- \approx k_0/(1+M)$.[1] The Mach number M is defined as the relationship between the flow velocity (U_0) and the sound speed (c_0) $M = U_0/c_0$. The wavenumber is defined as $k_0 = \omega/c_0$, with $\omega = 2\pi f$, where f is the frequency. An additional correction of the upstream and downstream wave number, based on a quasi 2D approach, can be used for non space-uniform mean flow conditions.[6] Equation 3 can be further extended, for each side of the two-port system, for an overdetermined system of n microphones, as described in equation 4. The overdetermined formulation of equation 4 is advantageous, since the least squares solution of this system of equations, based on Moore-Penrose pseudo matrix inverse technique suppresses random errors, such as those generated by aerodynamic pressure fluctuations in the ducts, noise on the acquisition system and small measurement errors, consequently, it can significantly increase the signal-to-noise ratio.

$$\left\{ \begin{array}{c} p^{+}(f) \\ p^{-}(f) \end{array} \right\} = \left[\begin{array}{cc} e^{-jk^{+}z_1} & e^{jk^{-}z_1} \\ e^{-jk^{+}z_2} & e^{jk^{-}z_2} \\ \vdots & \vdots \\ e^{-jk^{+}z_n} & e^{jk^{-}z_n} \end{array} \right]^{\otimes} \left\{ \begin{array}{c} p'(z_1, f) \\ p'(z_2, f) \\ \vdots \\ p'(z_n, f) \end{array} \right\} \tag{4}$$

where $\otimes$ represents the Moore-Penrose pseudo matrix inverse operator and z_k the location of the k^{th} microphone with respect to the reference position.

C. The two-port matrix coefficients

At least two measurements are necessary to determine the scatter matrix coefficients of equation 1. There are three approaches to obtain the two port coefficients: the first consists of varying the position of the external sound source (two-source technique);[4,7] the second is using a different outlet impedance for each experiment (two-load technique);[8] and the third constitutes of adopting a combination of the two techniques. The later approach is used in this paper. The two port equation 1 can be written for m experiments as:

$$\left[\begin{array}{cc} T^{+}(f) & R^{-}(f) \\ R^{+}(f) & T^{-}(f) \end{array} \right] = \left[\begin{array}{cccc} p^{+}_{2,1}(f) & p^{+}_{2,2}(f) & \cdots & p^{+}_{2,m}(f) \\ p^{-}_{1,1}(f) & p^{-}_{1,2}(f) & \cdots & p^{-}_{1,m}(f) \end{array} \right] \left\{ \begin{array}{cccc} p^{+}_{1,1}(f) & p^{+}_{1,2}(f) & \cdots & p^{+}_{1,m}(f) \\ p^{-}_{2,1}(f) & p^{-}_{2,2}(f) & \cdots & p^{-}_{2,m}(f) \end{array} \right\}^{\otimes}. \tag{5}$$

Similarly the determination of the left and right running waves, a least squares strategy can be used to solve equation 5, to improve the signal to noise ratio, which represents an overdetermined system of m equations and four unknowns: T^{+}, T^{-}, R^{+} and R^{-}.

III. Indirect impedance determination with flow

A. Problem description

A rectangular duct with cross sectional dimensions $b \times h$ and length l, shown in figure 2, is considered. Inside the duct a uniform mean flow in the z-direction with a Mach number M is considered. All walls are assumed to be perfectly rigid, except for the lined wall, localized at the upper x-boundary ($x = b$). Outside the lined section, the hypothesis of acoustic plane wave propagation is assumed to be valid up to a maximum frequency $f < c_0/2h$, corresponding the first transversal resonance frequency of the duct. This frequency range can be further extended by reducing the tube cross section up to a limit where the contribution from the edges at the lower and upper part of the impedance sections affects the estimation of the actual acoustic impedance under grazing flow.

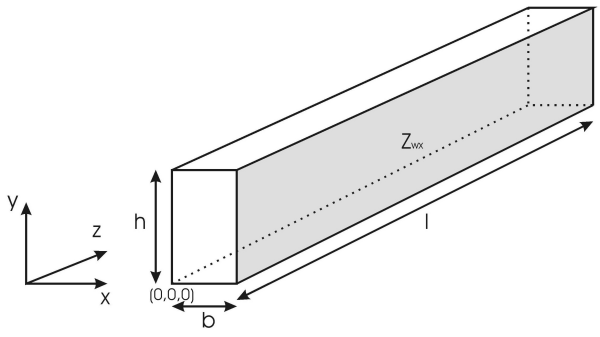

Figure 2. A rectangular duct with cross sectional dimensions $b \times h$ and length l with impedance Z_{wx} imposed on the boundary $x = b$.

B. Analytical two-port matrix formulation

The pressure field inside the single lined duct can be rewritten as a function of the right- and left-running acoustic waves propagating with the respective wavenumbers, k_z^+ and k_z^-:

$$p\left(x,y,z,t\right) = p^+\left(x,y,z,t\right) + p^-\left(x,y,z,t\right) = \left(A\left(x,y\right)e^{-jk_z^+ z} + B\left(x,y\right)e^{jk_z^- z}\right)e^{j\omega t} \tag{6}$$

where $A(x,y)$ and $B(x,y)$ represent the amplitude and the cross-sectional variation of the pressure fluctuations for, respectively, the right- and left-running acoustic waves. Applying the linearized momentum equation:

$$\rho_0 \frac{Du_z}{Dt} + \frac{\partial p}{\partial z} = \rho_0 \frac{\partial u_z}{\partial t} + Z_0 M \frac{\partial u_z}{\partial z} + \frac{\partial p}{\partial z} = 0 \tag{7}$$

with ρ_0 the mean density, $Z_0 = \rho_0 c_0$ the air characteristic acoustic impedance and $M = U_0/c_0$ the mean flow Mach number, in the lined section. The axial velocity fluctuation u_z for the right- and left-running acoustic waves are then determined as:

$$u_z\left(x,y,z,t\right) = u_z^+\left(x,y,z,t\right) + u_z^-\left(x,y,z,t\right) = \left(\frac{1}{Z^+}A\left(x,y\right)e^{-jk_z^+ z} - \frac{1}{Z^-}B\left(x,y\right)e^{jk_z^- z}\right)e^{j\omega t} \tag{8}$$

where Z^+ and Z^- are defined as:

$$Z^+ = Z_0\left(\frac{k_0 - Mk_z^+}{k_z^+}\right) \qquad\qquad Z^- = Z_0\left(\frac{k_0 + Mk_z^-}{k_z^-}\right) \tag{9}$$

Eliminating the propagation constants $A(x,y)$ and $B(x,y)$, and relating the acoustic pressure and velocity at the upstream ($z=0$) and downstream ($z=l$), leads to the following transfer matrix formulation:

$$\left\{\begin{array}{c} p\left(l\right) \\ u_z\left(l\right) \end{array}\right\} = \left\{\begin{array}{cc} \frac{Z^+e^{-jk_z^+ l} + Z^-e^{jk_z^- l}}{Z^+ + Z^-} & \frac{Z^+Z^-\left(e^{-jk_z^+ l} - e^{jk_z^- l}\right)}{Z^+ + Z^-} \\ \frac{e^{-jk_z^+ l} - e^{jk_z^- l}}{Z^+ + Z^-} & \frac{Z^-e^{-jk_z^+ l} + Z^+e^{jk_z^- l}}{Z^+ + Z^-} \end{array}\right\}\left\{\begin{array}{c} p\left(0\right) \\ u_z\left(0\right) \end{array}\right\} \tag{10}$$

Equation 10 can be compared with the experimentally or numerically obtained transfer matrix coefficients to determine the coefficients k_z^+ and k_z^-. This comparison leads to an overdetermined system with 4 equations and 2 unknowns which can be solved using a least square methodology.

C. Boundary conditions

The unknown impedance Z_{wx} is incorporated in the wavenumbers k_z^+ and k_z^- of equation 10. This is noticed by writing the cross-sectional variation of the three-dimensional acoustic pressure field of the right- and left-traveling waves inside the duct:

$$p^+\left(x,y,z,t\right) = C_z^+ e^{-jk_z^+ z}\left(e^{-jk_x^+ x} + C_x^+ e^{jk_x^+ x}\right)\left(e^{-jk_y^+ y} + C_y^+ e^{jk_y^+ y}\right)e^{j\omega t} \tag{11}$$

$$p^-\left(x,y,z,t\right) = C_z^- e^{jk_z^- z}\left(e^{-jk_x^- x} + C_x^- e^{jk_x^- x}\right)\left(e^{-jk_y^- y} + C_y^- e^{jk_y^- y}\right)e^{j\omega t} \tag{12}$$

where C_z^+, C_z^-, C_x^+, C_x^-, C_y^+ and C_y^- are propagation constants for the upstream and downstream propagating waves. For each cross-sectional mode (m,n), respectively, the x and y direction, the compatibility relationship gives an expression for the different wavenumbers in the $x-$, $y-$ and $z-$direction:

$$k_{z,m,n}^{+2} + k_{x,m}^{+2} + k_{y,n}^{+2} = \left(k_0 + Mk_{z,m,n}^+\right)^2 \tag{13}$$

$$k_{z,m,n}^{-2} + k_{x,m}^{-2} + k_{y,n}^{-2} = \left(k_0 - Mk_{z,m,n}^-\right)^2 \tag{14}$$

As the two-port methodology, adopted in present paper, relies on the hypothesis of plane acoustic wave propagation outside the lined section, only the least naturally attenuated mode ($m=n=0$) is considered. For this reason the subscripts are omitted in the remaining part of this paper.

Imposing the rigid wall boundary condition ($\partial p/\partial y = 0$) for $y = 0$ and $y = h$ in equation 11, the wavenumber in the $y-$direction for the upstream- and downstream-traveling acoustic waves is obtained ($k_{y,n}^{+} = k_{y,n}^{-} = n\pi/h$) and the y-dependency of the pressure field is expressed by an infinite summation of cosine functions:

$$e^{-jk_y^+ y} + C_y^+ e^{jk_y^+ y} = e^{-jk_y^- y} + C_y^- e^{jk_y^- y} = \sum_{n=0}^{\infty} cos\frac{n\pi y}{h}. \tag{15}$$

For the $(0,0)$ mode, it is thus possible to determine the wavenumbers in the x-direction k_x^+ and k_x^- as:

$$k_x^+ = \sqrt{\left(k_0 + Mk_z^+\right)^2 - k_z^{+2}} \qquad\qquad k_x^- = \sqrt{\left(k_0 - Mk_z^-\right)^2 - k_z^{-2}} \tag{16}$$

Applying to the equations 11 and 12 the right wall boundary condition ($\partial p/\partial x = 0$) at $x = 0$ results in $C_x^+ = C_x^- = 1$. Combining these equations with the linearized momentum equation 7, in the $x-$ direction, the following relations are obtained for the acoustic velocity fluctuations on the upstream and downstream directions:

$$u_x^+ = \frac{C_z^+}{Z_0}\frac{k_x^+}{k_0}\frac{1}{\left(1 - M\frac{k_z^+}{k_0}\right)}\left(e^{-jk_x^+ x} - e^{jk_x^+ x}\right)\sum_{n=0}^{\infty} cos\frac{n\pi y}{h}e^{-jk_z^+ z}e^{j\omega t} \tag{17}$$

$$u_x^- = \frac{C_z^-}{Z_0}\frac{k_x^-}{k_0}\frac{1}{\left(1 + M\frac{k_z^-}{k_0}\right)}\left(e^{-jk_x^- x} - e^{jk_x^- x}\right)\sum_{n=0}^{\infty} cos\frac{n\pi y}{h}e^{jk_z^- z}e^{j\omega t} \tag{18}$$

The impedance boundary condition at $x = b$ is based on the assumption that at this boundary the fluid particle displacement ζ and the wall particle displacement are identical. The acoustic impedance of the boundary and the velocity in the x-direction inside the duct are related to the particle displacement by:

$$\frac{p}{Z_{wx}} = \frac{\partial \zeta}{\partial t} \qquad\qquad u_x = \frac{D\zeta}{Dt} \tag{19}$$

The Ingard-Myers boundary condition formulation[9,10] is obtained by eliminating the particle displacement at $x = b$, which results in:

$$\frac{Dp\left(b,y,z,t\right)/Dt}{\partial u_x\left(b,y,z,t\right)/\partial t} = Z_{wx} \tag{20}$$

Combining the equations 11, 17 and 20 (or 12, 18 and 20) gives the solution for the unknown impedance at $x = b$ where k_z^+ and k_z^- are obtained from the two-port determination and k_x^+ and k_x^- from the compatibility relation 16:

$$Z_{wx} = jZ_0\frac{k_0}{k_x^+}\left(1 - M\frac{k_z^+}{k_0}\right)^2 cot\left(k_x^+ b\right) = jZ_0\frac{k_0}{k_x^-}\left(1 + M\frac{k_z^-}{k_0}\right)^2 cot\left(k_x^- b\right) \tag{21}$$

D. The rigid-/impedance-wall transition

The analytical formulation discussed above does not take into account the transition between the hard wall and the soft wall. Further research is still needed to gain additional insight in the physical phenomena that occur in this transition region[3] and how to incorporate this in the impedance eduction methodology. Rienstra[11] presents a Wiener-Hopf based analytical analysis of the scattered modes, in the transition region, however, to incorporate this approach in an impedance eduction methodology is rather cumbersome. This is caused by the fact that a preliminary knowledge of the impedance is needed and the fact that an automatic procedure is difficult to be developed due to the case-dependent determination of the integration path.

In this paper, the rigid-/impedance wall transition effects are incorporated in the impedance eduction approach by adding an infinitesimal transition element on both sides of the lined section, which behaves as an additional two-port element with a transfer matrix T_{tr}. Figure 3 illustrates this approach.

Assuming a continuity of pressure and axial velocity, at the various interfaces, the two-port pressure and velocity relationships can be written:

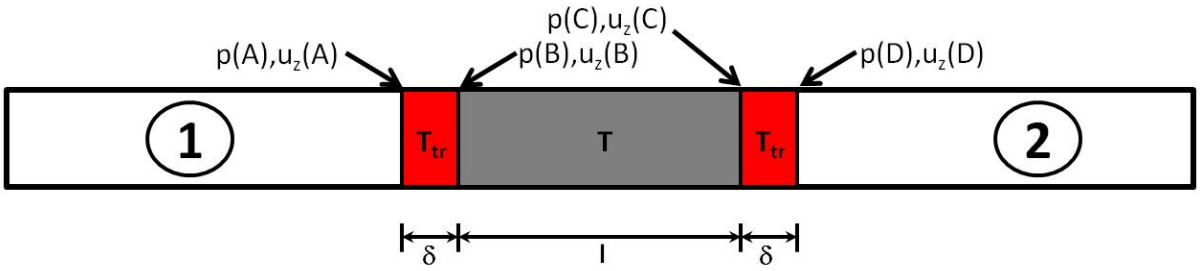

Figure 3. Impedance transition scheme.

$$\left\{ \begin{array}{c} p(A) \\ u_z(A) \end{array} \right\} = T_{tr} \left\{ \begin{array}{c} p(B) \\ u_z(B) \end{array} \right\} \tag{22}$$

$$\left\{ \begin{array}{c} p(B) \\ u_z(B) \end{array} \right\} = T \left\{ \begin{array}{c} p(C) \\ u_z(C) \end{array} \right\} \tag{23}$$

$$\left\{ \begin{array}{c} p(C) \\ u_z(C) \end{array} \right\} = T_{tr}^{-1} \left\{ \begin{array}{c} p(D) \\ u_z(D) \end{array} \right\} \tag{24}$$

which can be simplified to the relationship:

$$\left\{ \begin{array}{c} p\,(l) \\ u_z\,(l) \end{array} \right\} = T_{tot} \left\{ \begin{array}{c} p\,(0) \\ u_z\,(0) \end{array} \right\} = T_{tr} \times T \times T_{tr}^{-1} \left\{ \begin{array}{c} p\,(0) \\ u_z\,(0) \end{array} \right\} \tag{25}$$

where T is the matrix to be compared with the analytical formulation of equation 10 and T_{tr} is the matrix which contains the influence of the transition phenomena. The matrix T_{tr} adds four additional unknowns to the system of equations thus requiring a minimum of two extra simulations/measurements for its determination.

E. Impedance determination procedure

Equations 10, 16, 21 and 25 result in a system with a minimum 12 equations and 9 unknowns (k_z^+, k_z^-, k_x^+, k_x^-, Z_{wx} and the four T_{tr} elements), which can be solved by a least square strategy. The problem is simplified for the no-flow case, since $k_z^+ = k_z^-$, $k_x^+ = k_x^-$ and T_{tr} assumes a centrosymmetric matrix form, leading to a system with 8 equations and 5 unknowns.

The algorithm for impedance deduction, adopted in the present paper, executes the following steps:

1. If the impedance eduction is based on experimental data (section V case), execute the Fast Fourier Transform (FFT) to obtain the microphone's acoustic pressure in the frequency domain. If the impedance eduction is executed based on results from a finite element analysis (case studied in section IV) no Fourier Transform is necessary, since the input data is already calculated in the frequency domain;

2. For each side of the two-port system, use the equation 4 to calculate the downstream and upstream propagating waves (p^+ and p^-), and with the relations 3 and 8 calculate $p(A)$, $u_z(A)$, $p(D)$ and $u_z(D)$;

3. Given an expected impedance value, estimate an initial guess for the $k_x^\pm$ and $k_z^\pm$ using the equation 16 and 21, in addition, initialize the matrix T_{tr} as an identity matrix;

4. Calculate the total transmission matrix $T_{tot} = T_{tr} \times T \times T_{tr}^{-1}$;

5. Using the each measured/computed $p(A)$ and $u_z(A)$, following the formulation of equation 25, form a system of $2n$ equations to calculate $p(D)$ and $u_z(D)$ for each computation/simulation, where n is the number of experiments/simulations. Notice that for a flow case it is necessary at least 6 experiments for a determined system;

6. Adopting the Matlab® *fsolve* routine (for non linear system of equations solution) solve the system of equations, formed on the previous step, for the 6 unknowns;

7. With the $k_z^{\pm}$ determined in the previous step, use relation 16 to obtain the $k_x^{\pm}$ and

8. Finally use the equation 21 to calculate the impedance.

IV. Numerical validation

A. Numerical model description

A straight rectangular duct, with length, width and height, respectively: 1 m, $h = 0.10$ m, and $b = 0.05$ m, is chosen for the present validation. This geometry leads to a cut-on frequency of the transversal duct modes ($n = 1$) equal to 1700 Hz. To include the rigid-/impedance wall transition effects, a rigid wall of 0.25 m length is added at the inlet and outlet of the tube, consequently, the lined section has length of $l = 0.5$ m and is localized on the central part of the duct, as shown in figure 4. For meshing this geometry, a uniform structured hexahedral mesh is adopted. To ensure a minimal resolution of at least 10 points per wavelength, for the highest frequency of interest (1700 Hz), the side of each hexahedral element equals 5 mm, these parameters lead to an acoustical mesh containing 40000 elements.

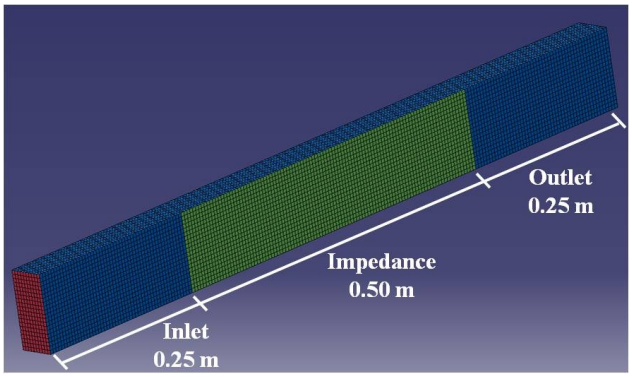

Figure 4. Representation of the finite element mesh and boundary conditions.

The acoustic finite element software LMS/Virtual Lab® Rev 9.0 is used to calculate the acoustic field. All walls are considered to be perfectly rigid, except for the region where the impedance is imposed. The inlet is considered anechoic, submitted to excitation source modeled as a pulsating panel. The outlet is defined as a wall with varying impedance values dependent on each simulation, in order to obtain a variable loading case.[8] On the wall side where the impedance is applied two different values are investigated: a $4Z_0$ frequency independent impedance, and a frequency dependent impedance obtained using the Extended Helmholtz Resonator Model.[12] In the simulations, in order to trigger more remarkable hard wall soft wall transition effects, the input parameters are chosen in order to generate the highest possible impedance values, for a wide range of frequencies, within the validity of the model, to generate a realistic impedance values. For both the frequency dependent and the frequency independent impedance simulations, a no-flow case (M=0) and a uniform mean flow case (M=0.3) are studied.

B. Discussion of the results

1. *No-flow cases*

The outcome of impedance eduction based on the finite element results is shown on figure 5 and 6, respectively, for the frequency independent and dependent impedance cases.

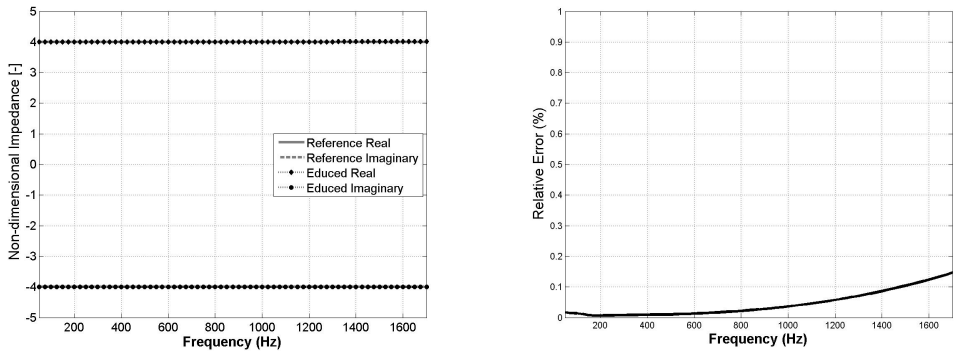

Figure 5. Comparison between the frequency independent imposed and the educed impedance (left), and the relative error between these two impedances (right) (M=0).

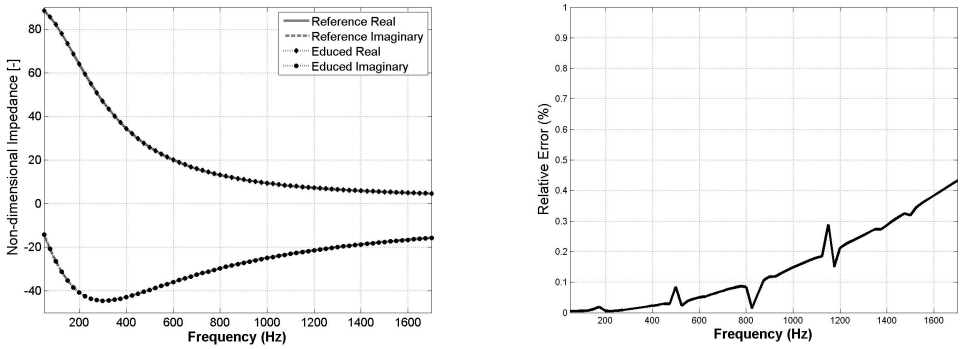

Figure 6. Comparison between the frequency dependent imposed and the educed impedance (left), and the relative error between these two impedances (right) (M=0).

In figures 5 and 6, the left images correspond to the comparison between the imposed impedance on the finite element model and the one educed by the present method. The right images present the relative error between these two impedances, defined as the modulus of the relative difference between the two values.

In both figures an excellent agreement between the imposed and the educed acoustic impedance is observed. The error grows following a exponential rule until the tube cut-on frequency. This behavior is because, as the frequency grows, the acoustic plane wave propagation hypothesis becomes less valid. Some spikes are noticed on the error curve of figure 6, these are originated from local numerical instabilities in the optimization routine used. This problem affects only few points in the frequency spectrum and does not jeopardize the overall accuracy of the solution.

2. Flow cases

Figures 7 and 8 present the results for the frequency independent and dependent imposed impedance, respectively, for a medium with a uniform mean flow with Mach number equal to 0.3. In these figures, the left image represents the comparison between the imposed and the educed impedance and the right image represents the relative error between these two values.

The flow case results presented in figure 7 and 8 also show an excellent agreement between the imposed and the educed impedance. The relative error is slightly higher than for the no-flow cases. Similar for the no flow case, the error grows with increasing frequency, for both test cases, following an exponential pattern.

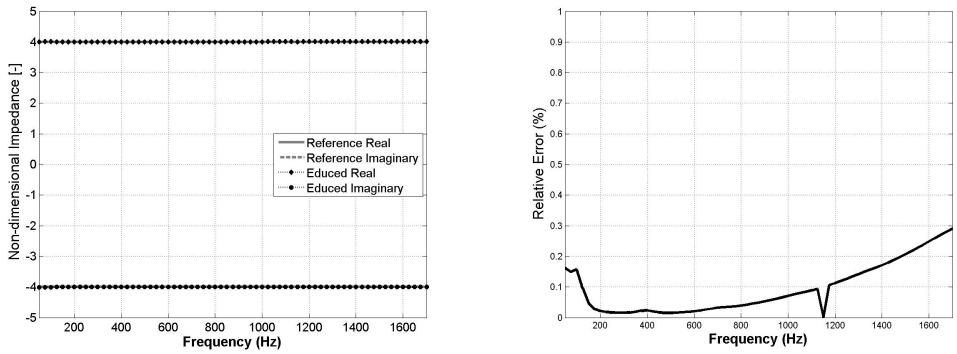

Figure 7. Comparison between the frequency independent imposed and the educed impedance (left), and the relative error between these two impedances (right) (M=0.3).

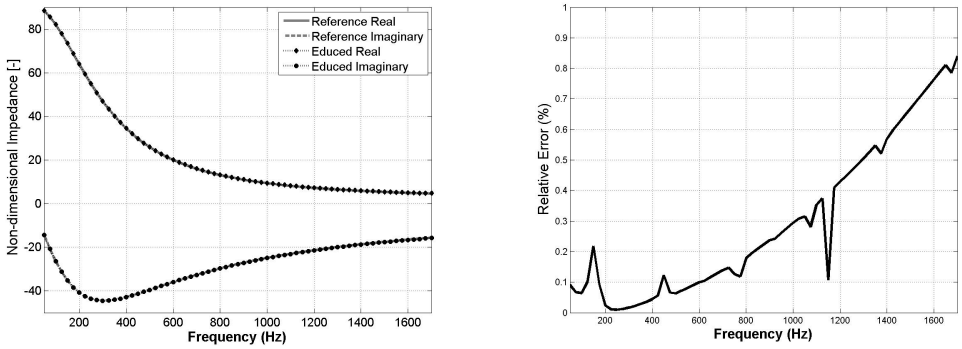

Figure 8. Comparison between the frequency dependent imposed and the educed impedance (left), and the relative error between these two impedances (right) (M=0.3).

V. Experimental set-up and results

A. The experimental facility

An open aeroacoustic test rig, described by De Roeck and Desmet,[13] is used for the present measurements. This test facility allows an analysis of the aeroacoustic noise generation, absorption and propagation mechanisms for subsonic flow applications under various mean flow conditions. Figure 9 presents the schematic view of the open flow circuit testing section, the test rig adopted for this paper.

In the present experiments, 4 microphones are used on each side of the two-port system, the sampling frequency is 25 kHz. As excitation signal a sweep sine is chosen, which has a total duration of 20 seconds and frequency range between 20 Hz to 3.5 kHz. For the no-flow cases a sampling time of 60 seconds is chosen, by turn, for the flow cases a sampling time of 600 seconds is used. In order to ensure a good signal to noise relationship, the loudspeakers were adjusted to guarantee, at the sample position, a sound pressure level close to 120 dB, for the all excitation frequency range. The Mach number equals 0, 0.1 and 0.17, where the later corresponds to the maximum reachable flow speed for the test section of the experimental flow facility. For accuracy, the calculated, not the measured Mach number was adopted for the impedance eduction calculation, what leads to a slight variation of the actual Mach number used for impedance eduction and the expected Mach number value.

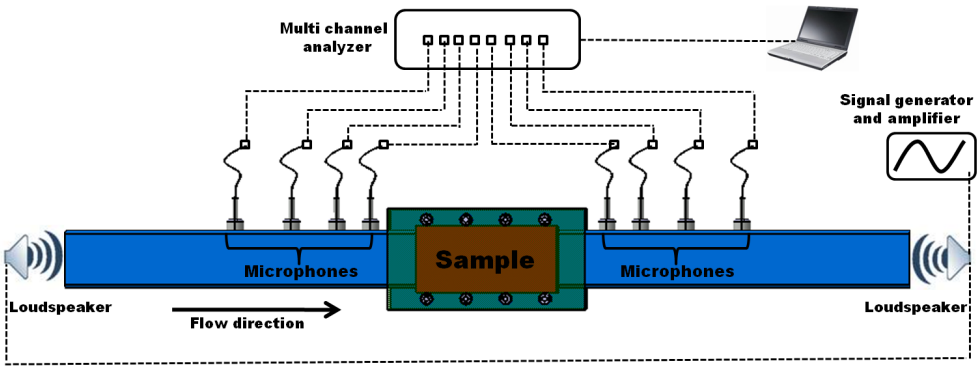

Figure 9. Schematic representation of the experimental rig.

B. The analyzed samples

Two acoustic liner samples, which were previously studied by Busse et al.,[14] are tested in this paper. In Busse et al. the acoustic impedance results are determined by comparing insertion loss measurements with a numerical optimization based on the Extended Helmholtz Resonator Model.[12] The same sample notation of Busse et al. is adopted in this paper and their results are denoted as the reference. The physical properties of these samples are presented in table 1 and the pictures of the sample, from Busse et al.,[14] are shown on figure 10.

Table 1. Main geometric parameters of the analyzed liners samples.

Test object	Sample 1	Sample 2
Identification:	Perforated Liner SDOF	Linear Liner SDOF
Type:	Single Degree of Freedom	Single Degree of Freedom
Cell depth:	0.5 in (12.7 mm)	1.21 in (30.73 mm)
Hole diameter:	1.45 to 1.5 mm	1.1 mm covered by a wire mesh
Hole placement:	Parallel	N/A
Porosity:	≈ 4 %	N/A
Open area ratio:	≈ 4.3 %	N/A
$\lambda/4$ resonance:	≈ 6752 Hz	≈ 2790 Hz
Helmholtz resonance:	≈ 1670 Hz	≈ 623 Hz

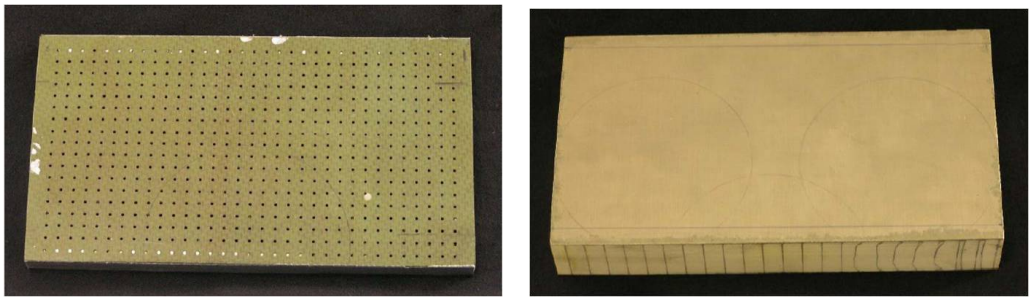

Figure 10. Test samples. Left: sample number 1 - perforated liner with single degree of freedom; Right: sample number 2 - linear liner with single degree of freedom.

Sample 1 corresponds to an acoustic liner which is typically installed in narrow body aircrafts, this

sample is of particular interest for aeronautical engineering applications. Sample number 2 is important to be analyzed because its close to linear behavior, generated by the wire-mesh covering. In this paper, both samples are tested for Mach number of 0, 0.1 and 0.17.

C. Discussion of the experimental results

1. Sample 1

A comparison between the reference result and the educed impedance, using the present technique, is shown in figure 11. The figure 12 presents the relative difference between the reference and the educed results.

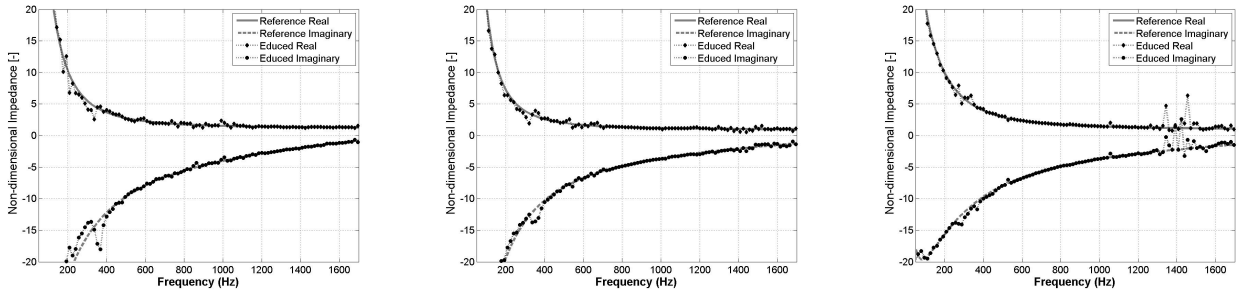

Figure 11. Comparison between the reference results and the impedance educed by the present technique for sample 1. (Left M=0, center M = 0.1 and right M = 0.17.)

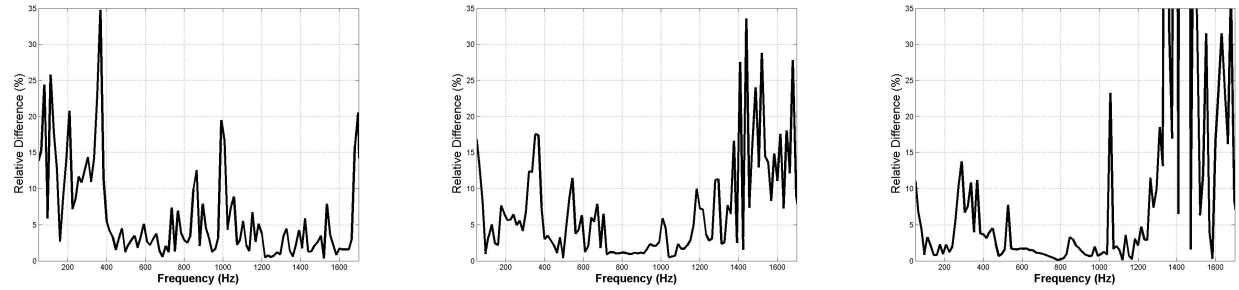

Figure 12. Relative difference between the reference impedance and the educed impedance by the present technique for sample 1. (Left M=0, center M = 0.1 and right M = 0.17.)

From the figures 11 and 12 a good agreement between the reference solution and the educed one is observed. The educed solution is less smooth than the reference one, because the present technique does not adopt an impedance model, while the Busse et al.[14] results are based on optimizing the coefficients for the Extended Helmholtz Resonator Model. From the figures, it is noticed that for higher frequencies additional oscillations occur which do not smooth out with a higher sampling time (and the consequent increased number of averages). It is observed that for the no flow case it is barely noticeable oscillations, while for the case with Mach number equal 0.17 these oscillations are much more pronounced. This might indicate that the flow is interacting with the liner surface cavities generating a whiling phenomena, which jeopardizes the hypothesis of no significant noise generation in the interior of the two-port system.

2. Sample 2

Figure 13 plots the educed impedance against the reference values for the sample 2, and figure 14 shows the relative difference for the same sample.

Also for this sample, a good agreement between the reference impedance values and the educed results is observed. It is noticed that the educed impedance curve shows less oscillations of the solution related to the wire-mesh that covers this sample. Opposite to sample 1, there is less flow penetration in the liner

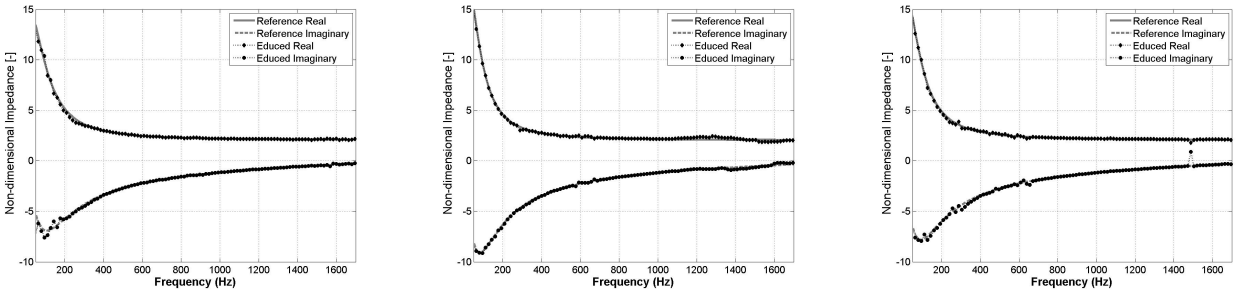

Figure 13. Comparison between the reference results and the impedance educed by the present technique for sample 2. (Left M=0, center M = 0.1 and right M = 0.17.)

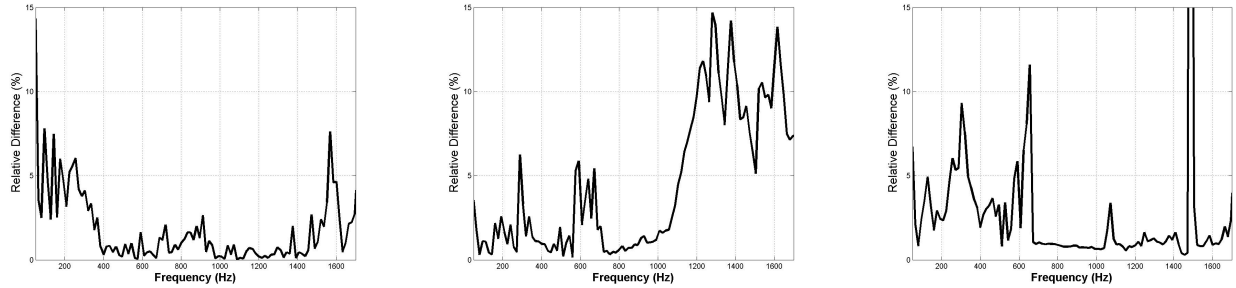

Figure 14. Relative difference between the reference impedance and the educed impedance by the present technique for sample 2. (Left M=0, center M = 0.1 and right M = 0.17.)

cavities and consequently no whistle like noise generation in its cavities. Observing the results at Mach 0.17 it is noticed that for frequency equal to 1500 Hz, a peak in the educed impedance solution is presented, this corresponds to a single frequency where no solution was found by the system of equations. As this only a local phenomenon, this does not arise a major problems about the validity of the methodology.

VI. Impedance eduction issues

For an accurate impedance eduction, some parameters should be taken into account and carefully determined. Based on the authors' experience, the most influencing parameters are: the rigid-/impedance wall transition; the flow Mach number determination; the microphones positioning and the sampling time/number of averages. In this section, only the experimental results at Mach 0.1 for the sample 2 are considered, and all numerical cases are presented for frequency dependent impedance with Mach 0.3.

A. The rigid-/impedance-wall transition effects on the educed impedance

One of the most significant influences on the impedance eduction results is the transition between the rigid and the impedance wall. Figure 15 presents, on the left image, the educed impedance when the transition is taken into account and the right image shows the case where this effect is not considered.

From the results of figure 15, it is noticeable that the acoustic scattering caused by the transition between the rigid and the impedance wall plays an important role for all frequencies in the analyzed range.

Similar transition effects are noticed for finite elements simulations. Figure 16 presents the effects of not taking into account the impedance transition in the impedance eduction methodology. The left image corresponds to the reference result, where the rigid-/impedance wall transition effects are taken on account, and the right image is the case where this effect is not considered.

Figure 16 proves that oscilations on the educed impedance are caused by the sudden jump of impedance

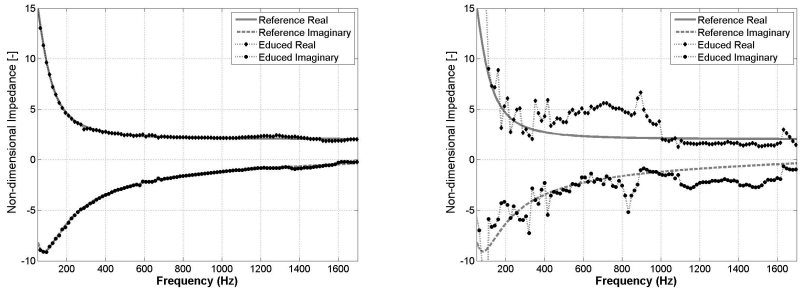

Figure 15. Rigid-/impedance wall transition effects on an experimental case. Reference result (left) with the rigid-/impedance wall effect taken on account, and without the impedance transition effect taken on account (right). Results for sample 2 and M = 0.1.

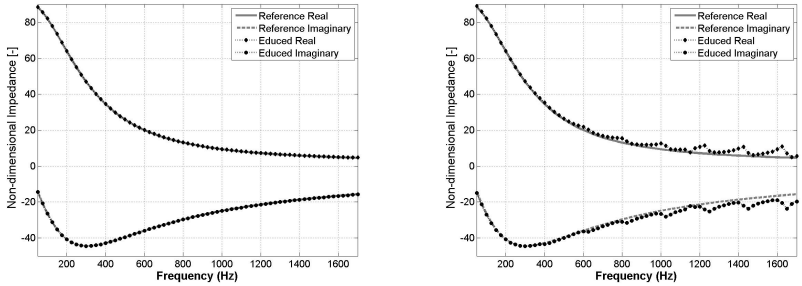

Figure 16. Rigid-/impedance wall transition effects for the numerical frequency dependent impedance eduction. Reference result (left) with the rigid-/impedance wall effect taken on account, and without the impedance transition effect taken on account (right). Results for potential flow with M = 0.3.

on the beginning and end of the liner sample.[15] In a future work, it is planed to execute simulations that reproduce the geometry and the wall imposed impedance cases, in order to verify if the impedance transition coefficients are the same.

B. The influence of the Mach number

The correct flow Mach number is an important parameter to be determined for precise impedance eduction results. Figure 17 illustrates this effect for a variation of 10% on the correct Mach number.

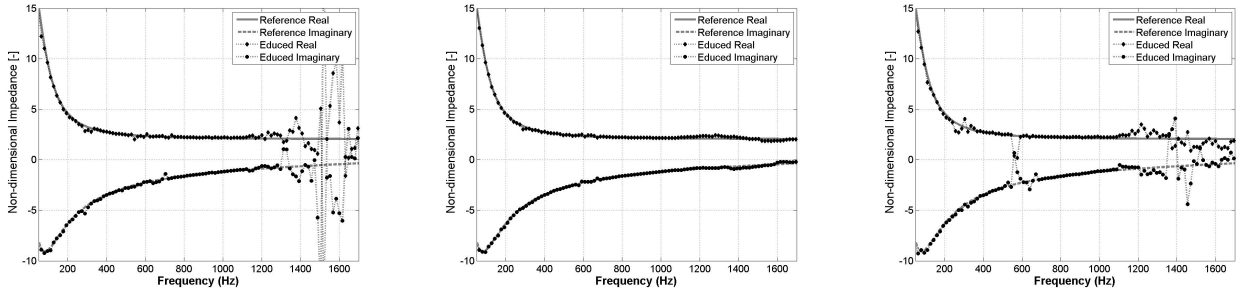

Figure 17. Impedance eduction for erroneous Mach numbers (left M=0.9, center M=0.1 and right M=0.11).

When comparing the results of the figure 17, it is noticed that an error of 10% on the Mach number determination, seriously compromises the accuracy of the solution, mainly at higher frequencies. As to

measure the flow Mach number accurately in the tube section is a cumbersome task, in this paper it was preferred to calculate this value based on the 4 microphone data on each side of the two port system and then execute an average between the two obtained values.

C. Influence of the microphone position

The microphone position also plays an important role in the correct impedance eduction. For the microphone localization determination an indirect distance measurement is preferred. Boonen et. al[16] present a suitable technique that, with small modifications on the rig setup, permits accurate microphone position determination. For the present experiment, the uncertainties are presented in table 2. In this table, the microphone numbering is determined growing from the center of the testing section (where the sample is localized) to the borders, where the microphones, localized on the right side of the sample, represent the microphones 1 to 4, and the microphones on the left side of the sample correspond to the microphones 6 to 9.

Table 2. Microphone positions and respective errors on positioning.

Microphone number	Position (mm)	Uncertainty $\pm\delta$(mm)
1	-335.0	0.8
2	-416.0	1.2
3	-548.0	1.5
4	-760.0	2.0
6	553.0	0.7
7	634.0	1.4
8	765.0	1.7
9	977.0	2.0

For the study of the influence of the microphone position on the impedance eduction results, considering that each microphone is localized on a position z_i, where i corresponds to the microphone number. A first analysis assumes all microphones positions on $z_i - \delta$, and in a second situation all the microphones adopted to be in $z_i - \delta$. Figure 18 presents this analysis results, where the left image corresponds to the case $z_i - \delta$, the central image corresponds to the impedance educed with the microphones on the reference position z_i and the right image corresponds to the calculation where the microphones position is considered to be $z_i + \delta$.

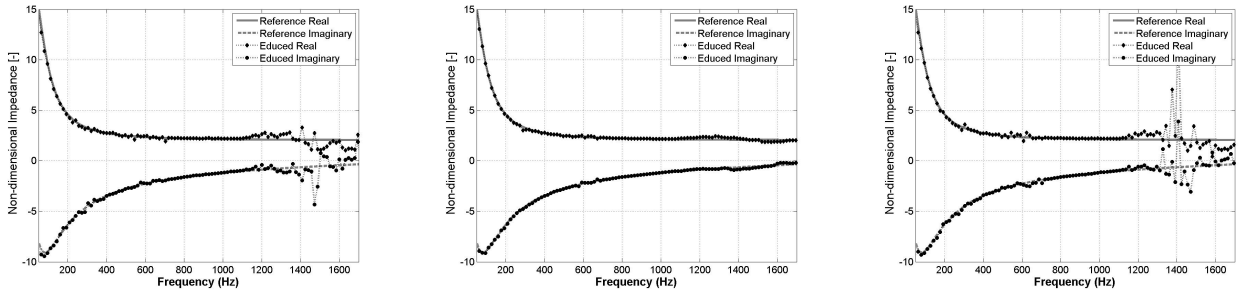

Figure 18. Impedance eduction for different microphone position. Where the left image corresponds to $z_i - \delta$, the center image is the reference, and the right image corresponds to $z_i + \delta$. (Sample 2, M=0.1)

Figure 18 shows that small microphone positioning variations, even inside the uncertainty boundaries of the position measurement, cause significant effects on the educed impedance, mainly at higher frequencies.

D. Influence of the sampling time

Another important parameter to be controlled in impedance eduction experiments is the sampling time. Figure 19 shows a comparison of results for data sampled at the same sampling frequency and FFT processed

with the same block size, but, with increasing sampling time of 120 s, 240 s, 480 s and 600 s, from the left to the right image, respectively.

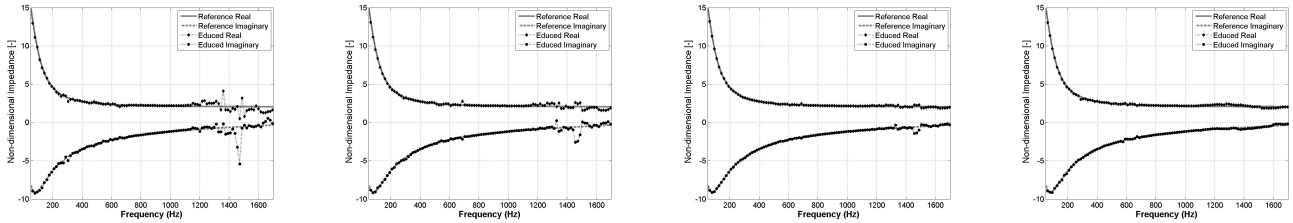

Figure 19. Impedance eduction for different sampling times. From the left to the right the images corresponds, respectively, to 120 s, 240 s, 480 s and 600 s. (Sample 2, M=0.1).

The results of figure 19 show that the most critical influence of the sampling time, on the educed impedance, is noticed at higher frequencies. As the sampling time increases, the number of averages proportionally grows, consequently, the random errors are smoothed out from the solution. For the present configuration, a sampling time of 600 seconds is determined to be large enough to smooth out the random errors and lead to a solution which converges in time.

VII. Conclusions

In this paper, an analytical technique for the acoustic impedance eduction is presented, numerically validated and applied to experiments. A sensitivity analysis of the effect of the input parameters (rigid-/impedance wall transition, Mach number, sample time and microphone positioning) on the educed impedance is presented. The analytical technique relies on the acoustic plane wave propagation hypothesis where the acoustic waves are propagated with frequency range below the cut-on frequency of the transversal duct modes ($n = 1$). The present methodology is advantageous when compared with concurrent techniques due the reduced number of pressure sensors necessary for data acquisition and non-destructiveness of the sample. The validation shows an excellent agreement between the finite element model imposed impedance and the educed impedance by the present technique. The experimental results are in good agreement with results calculated by an independent methodology, on a different test rig. The sensitivity analysis on the input parameters shows that the rigid-/impedance wall transition effects must be taken to account for a precise liner sample impedance eduction, in addition the flow Mach number and the microphone positioning should be carefully determined and a higher enough sampling time should be considered to improve the accuracy at higher frequencies.

Acknowledgments

Leandro D. Santana acknowledges the financial support of the European Commission through the Marie-Curie Research and Training Network "AETHER", Contract Nr. MRTN-CT-2006-035713. The authors acknowledge Alenia Aermacchi S.p.A. for the supply of the samples analyzed in this paper.

References

[1]Elnady, T. and Bodén, H., "An Inverse Analytical Method for Extracting Liner Impedance from Pressure Measurements," *10th AIAA/CEAS Aeroacoustics Conference*, No. AIAA 2004-2836, 2004.

[2]Dean, P., "An in situ method of wall acoustic impedance measurement in flow ducts," *Journal of Sound and Vibration*, Vol. 34, No. 1, 1974, pp. 97 – 130.

[3]Gabard, G., "Mode-Matching Techniques for Sound Propagation in Lined Ducts with Flow," *16th AIAA/CEAS Aeroacoustics Conference*, No. AIAA 2010-3940, 2010.

[4]Åbom, M., "Measurement of the scattering-matrix of acoustical two-ports," *Mechanical Systems and Signal Processing*, Vol. 5, No. 2, 1991, pp. 89 – 104.

[5]De Roeck, W., *Hybrid Methodologies for the Computational Analysis of Confined Subsonic Flows*, Ph.D. thesis, Katholieke Universiteit Leuven, 2007.

[6]Dokumaci, E., "On the Propagation Of Plane Sound Waves in Ducts Carrying an Incompressible Axial Mean Flow Having

an arbitrary velocity Profile," *Journal of Sound and Vibration*, Vol. 249, No. 4, 2002, pp. 824 – 827.

[7]Munjal, M. L. and Doige, A. G., "Theory of a two source-location method for direct experimental evaluation of the four-pole parameters of an aeroacoustic element," *Journal of Sound and Vibration*, Vol. 141, No. 2, 1990, pp. 323 – 333.

[8]Lung, T. Y. and Doige, A. G., "A time-averaging transient testing method for acoustic properties of piping systems and mufflers with flow," *The Journal of the Acoustical Society of America*, Vol. 73, No. 3, 1983, pp. 867–876.

[9]Ingard, U., "Influence of Fluid Motion Past a Plane Boundary on Sound Reflection, Absorption, and Transmission," *The Journal of the Acoustical Society of America*, Vol. 31, No. 7, 1959, pp. 1035–1036.

[10]Myers, M., "On the acoustic boundary condition in the presence of flow," *Journal of Sound and Vibration*, Vol. 71, No. 3, 1980, pp. 429 – 434.

[11]Rienstra, S., "Acoustic scattering at a hard-soft lining transition in a flow duct," *Journal of Engineering Mathematics*, Vol. 59, 2007, pp. 451–475, 10.1007/s10665-007-9193-z.

[12]Rienstra, S. W., "ImpedanceModels in Time Domain including the Extended Helmholtz Resonator Model," *12th AIAA/CEAS Aeroacoustics Conference*, 2006.

[13]De Roeck, W. and Desmet, W., "Experimental acoustic identification of flow noise sources in expansion chambers," *Proceedings of ISMA 2008*, 2008, pp. 455 – 470.

[14]Busse, S., Richter, C., Thiele, F. H., Heuwinkel, C., Enghardt, L., Röhle, I., Michel, U., Ferrante, P., and Scofano, A., "Impedance Deduction Based on Insertion Loss Measurements of Liners under Grazing Flow Conditions," *14th AIAA/CEAS Aeroacoustics Conference (29th AIAA Aeroacoustics Conference)*, No. AIAA 2008-3014, May 2008.

[15]De Roeck, W. and Desmet, W., "Indirect acoustic impedance determination in flow ducts using a two-port formulation," *15th AIAA/CEAS Aeroacoustics Conference (30th AIAA Aeroacoustics Conference)*, No. AIAA 2009-3302, May 2009.

[16]Boonen, R., Sas, P., Desmet, W., Lauriks, W., and Vermeir, G., "Calibration of the two microphone transfer function method with hard wall impedance measurements at different reference sections," *Mechanical Systems and Signal Processing*, Vol. 23, No. 5, 2009, pp. 1662 – 1671.